JACS
JOURNAL OF THE AMERICAN CHEMICAL SOCIETY
Communication
pubs.acs.org/JACS

Polyaromatic Nanocapsules Displaying Aggregation-Induced Enhanced Emissions in Water

Yusuke Okazawa, Kei Kondo, Munetaka Akita, and Michito Yoshizawa*

Chemical Resources Laboratory, Tokyo Institute of Technology, 4259 Nagatsuta, Midori-ku, Yokohama 226-8503, Japan

Supporting Information

ABSTRACT: V-shaped polyaromatic amphiphiles with phenanthrene or naphthalene rings spontaneously and quantitatively formed micelle-like nanocapsules in water at room temperature. In contrast to usual polyaromatic aggregates with weak fluorescent properties, the new capsules providing spherical polyaromatic shells with diameters of ∼2 nm show strong fluorescent emissions due to an aggregation-induced enhanced emission (AIEE) effect and moreover encapsulate a fluorescent coumarin dye to generate highly emissive host−guest composites.

Photophysical properties of fluorescent organic molecules are greatly affected by the surroundings. Usually, fluorescent emissions of planar polyaromatic compounds are weakened or annihilated in the aggregate states (e.g., in concentrated solutions and the solid states) because of notorious aggregation-caused emission quenching (ACEQ) effects.[1] In contrast, aggregation-induced enhanced emission (AIEE) has been recently found in some nonplanar aromatic compounds, originating mainly from restricted intramolecular motion upon aggregation.[2] The development of novel AIEE-active composites is a fascinating area of recent research because of their promising applications in photonic biosensors and materials. Incorporation of AIEE units into functional polymers and oligomers is relatively explored,[2,3] whereas, to the best of our knowledge, successful preparation of fluorescent supramolecular capsules and cages[4−7] *with an AIEE effect* has not been reported so far. Herein we present new V-shaped polyaromatic amphiphilies **1a** and **1b** bearing phenanthrene and naphthalene rings, respectively, and the spontaneous and quantitative formation of micelle-like nanocapsules **2a**,**b** with spherical polyaromatic shells in water (Figure 1a). Notably, the polyaromatic capsules exhibit AIEEs with good photostability and encapsulate one molecule of fluorescent coumarin-102 dye through hydrophobic effects. The resultant host−guest composites display strong guest emissions through efficient fluorescence resonance energy transfer (FRET) upon irradiation of the host frameworks.

We have recently shown that anthracene-embedded amphiphile **1c**′ bearing two trimethylammonium groups (R = $-CH_2CH_2N(CH_3)_3^+ \cdot NO_3^-$) forms polyaromatic capsule **2c**′ with a diameter of ∼2 nm in an aqueous solution through aromatic−aromatic and hydrophobic interactions.[6a] The nanostructure acts as a fluorescent supramolecular host, but the emissive property of the capsule is considerably low as compared with that of the monomeric amphiphile owing to the typical ACEQ effect through intermolecular tight stacks between the anthracene fluorophores. Thus, we designed amphiphilic molecules **1a**,**b** by the replacement of the anthracene rings of **1c** by (i) less-symmetrical phenanthrene rings and (ii) smaller naphthalene rings. By changing the shape and size of the polyaromatic panels, we posited that *relieving strong aromatic−aromatic interactions* between the prototypical amphiphiles would prompt the formation of supramolecular capsules with high emissive properties. Molecular modeling study prior to synthetic experiments indicated that the polyaromatic frameworks of amphiphiles **1a**,**b** adopt distorted V-shaped conformations (Figure 1b) due to steric repulsions between the adjacent phenanthryl−phenyl rings on **1a** and naphthyl−phenyl rings on **1b** (with dihedral angles of 125.7° and 124.8°, respectively).

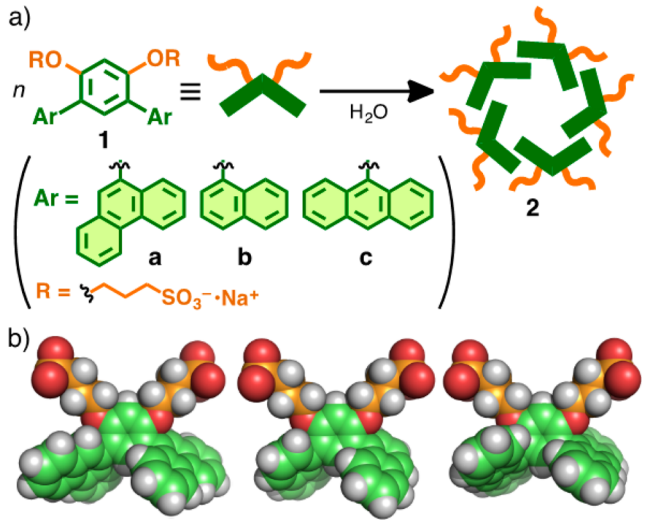

Figure 1. (a) Schematic representation of the formation of polyaromatic nanocapsules **2a**−**c** from amphiphilic molecules **1a**−**c**. (b) The optimized structures of **1a** (left), **1b** (center), and **1c** (right) without the counterions obtained by DFT calculations (B3LYP/6-31G(d,p) level).

Amphiphiles **1a**,**b** and **1c** as a reference compound were synthesized in four steps starting from 1,3-dimethoxybenzene.[8] The polyaromatic panels were introduced by Negishi coupling protocol and the sulfonate substituents (R = $-CH_2CH_2CH_2SO_3^- \cdot Na^+$) were employed as readily affordable, anionic hydrophilic groups. Stirring **1a**−**c** (2.0 mmol) in water (1.0 mL) at room temperature (for **1a**,**b**) or 80 °C (for **1c**)

Received: November 7, 2014
Published: December 22, 2014

DOI: 10.1021/ja511463k
J. Am. Chem. Soc. 2015, 137, 98−101

resulted in the spontaneous formation of nanocapsules **2a**–**c** within 1 min. NMR spectroscopy, dynamic light scattering (DLS) analysis, and atomic force microscopy (AFM) of **2a**–**c** confirmed the quantitative formation of spherical assemblies with core diameters of approximately 1–2 nm. In ^{1}H NMR spectra, the phenanthryl signals ($H_{c\text{-}k}$) of **2a** in D_2O were broadened and shifted upfield as compared with those of **1a** in CD_3OD (Figure 2a,b) due to the formation of an assembled

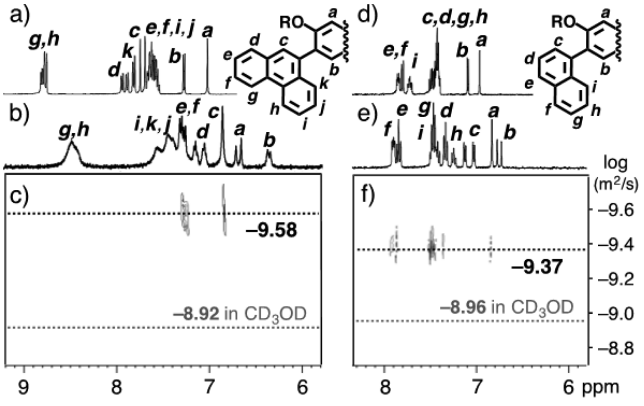

Figure 2. ^{1}H NMR spectra (400 MHz, r.t.) of amphiphilic molecules (a) **1a** and (d) **1b** in CD_3OD. ^{1}H NMR and DOSY spectra (400 MHz, 25 °C) of polyaromatic nanocapsules (b,c) **2a** and (e,f) **2b** in D_2O (2.0 mM based on **1a**,**b**).

structure with stacked polyaromatic panels. The prominent upfield shift of the signal for proton H_b ($\Delta\delta = -0.90$ ppm) on the central benzene ring indicates a capsular structure, in which the inner protons are efficiently shielded by the plural phenanthrene rings. However, shifts observed for the polyaromatic signals of **2b** in D_2O were smaller than those of **2a** in D_2O (Figure 2d,e). This observation is ascribed to a weak aromatic shielding effect of adjoining naphthalene rings in **2b**. The diffusion-ordered spectroscopy (DOSY) NMR spectra of **2a**–**c** exhibited single bands (Figures 2c,f and S49), and thus, the hydrodynamic diameters of the core structures were estimated to be approximately 1–2 nm.[9] The existence of such small assemblies in water was also confirmed by DLS analysis displaying particles with narrow size distributions (Figure S50a).

AFM study elucidated the spherical morphologies of **2a**–**c**. Aqueous solutions of **2a**–**c** (1.0 mM based on **1a**–**c**) were dropped on mica surfaces and subsequently dried in the air. AFM images of **2a**, **2b**, and **2c** showed spherical particles with the average diameters of 2.6 ± 0.9, 2.0 ± 0.6, and 2.2 ± 0.5 nm, respectively (Figures 3a–e and S50b), which are comparable to the outer diameters of pentameric spherical assemblies including the pendant sulfonate groups, as suggested by molecular modeling study (Figure 3f,g). Notably, the size of the obtained AIEE-active capsules is much smaller than that of the AIEE-active aggregates (>~30 nm) reported previously by other groups.[2,3] In short, we obtained the new nanocapsules with phenanthrene or naphthalene frameworks, whose size and shape are comparable to those of original **2c** with anthracene frameworks.

Photophysical properties of nanocapsules **2a**–**c** are highly dependent on the identity of the embedded polyaromatic fluorophores. In the UV–visible spectra in water, characteristic absorption bands of **2a**, **2b**, and **2c** appeared at λ_{max} = 297, 293, and 368 nm, respectively (Figure 4a), which are essentially the same as those of the corresponding amphiphilic molecules in CH_3OH (Figure S51). Although the fluorescent emission of

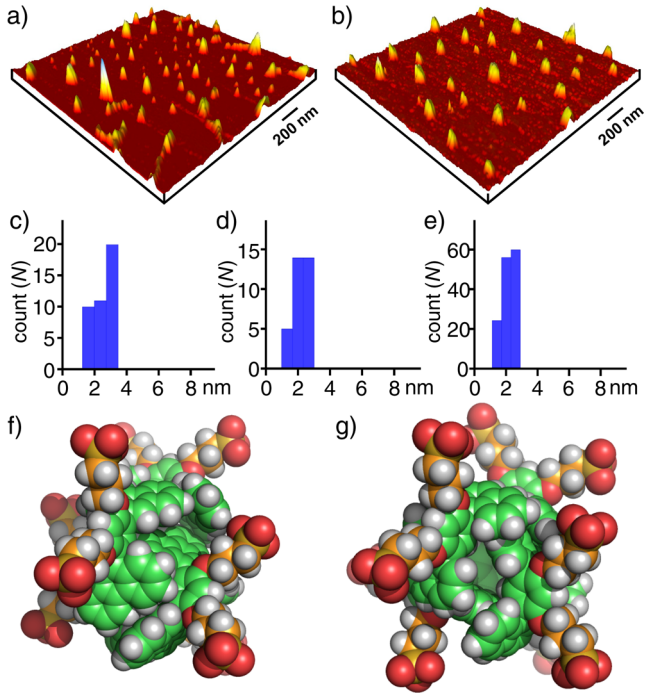

Figure 3. Structural analysis of polyaromatic nanocapsules **2a**–**c** by AFM. AFM images of (a) **2a** and (b) **2b** on mica. Size and number (N) distributions of the AFM images of (c) **2a**, (d) **2b**, and (e) **2c**. Molecular modeling of (f) **2a** and (g) **2b** composed of five molecules of **1a** and **1b**, respectively.

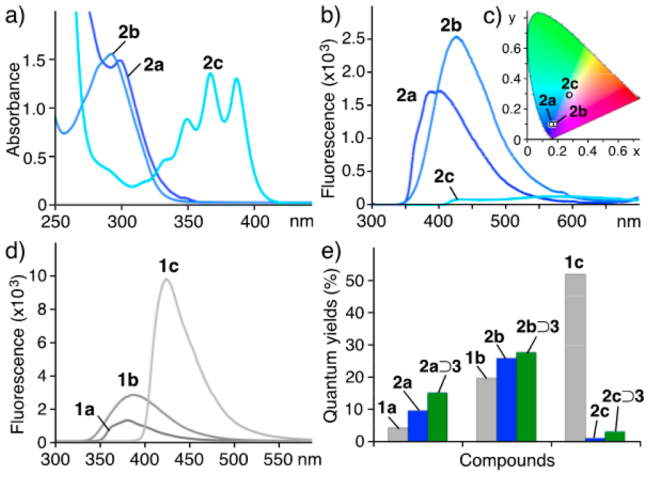

Figure 4. (a) UV–visible and (b) fluorescence spectra (r.t.) of **2a**–**c** in H_2O (1.0 mM based on **1a**–**c**). (c) CIE coordinate diagram of **2a**–**c**. (d) Fluorescence spectra (r.t.) of **1a**–**c** in CH_3OH (1.0 mM). (e) Quantum yields (%) of **1a**–**c**, **2a**–**c**, and **2a**–**c**⊃**3**. Excitation wavelengths: λ_{ex} = 297 nm for **1a**, **2a**, and **2a**⊃**3**, λ_{ex} = 293 nm for **1b**, **2b**, and **2b**⊃**3**, and λ_{ex} = 368 nm for **1c**, **2c**, and **2c**⊃**3**.

monomer **1c** is high in CH_3OH (Φ_F = 52%; Figure 4e), capsule **2c** showed a significantly broadened and weakened emission band (Φ_F = 1%) around 580 nm (Figure 4b), owing to the strong anthracene–anthracene interactions. In sharp contrast, new capsules **2a** and **2b** showed prominent emissions at λ_{max} = 400 and 424 nm, respectively, in water (Figure 4b). It is worthy of note that the emission quantum yields of **2a** and **2b** are 10- and 26-fold higher than that of **2c**, respectively (Figure 4e, blue bars). Moreover, the emission intensity of **2a** is 2.5-times higher than that of **1a** by an AIEE effect, but the emission of **2c** is 50-times

DOI: 10.1021/ja511463k
J. Am. Chem. Soc. 2015, 137, 98–101

weaker than that of **1c** by an ACEQ effect (Figure 4d,e). The observed AIEE effect was also supported by the fluorescence studies of **2a** and **2b** in H_2O/CH_3OH mixtures with different contents of water (Figure S53). The CIE coordinate diagram of micelles **2a**–**c** quantified the total fluorescent color (Figure 4c).

Improvement in photostability was obviously found for polyaromatic nanocapsules **2a**,**b**. The aqueous solutions of **2a**–**c** (1.0 mM based on **1a**–**c**) were irradiated by a xenon lamp (150 W m^{-2} without cutoff filters) at room temperature under air, and the variations of the emission intensities were monitored by fluorescence spectroscopy. As expected, the emission band derived from anthracene-embedded micelle **2c** (at 580 nm) decreased significantly upon light irradiation due to the usual photo-oxidization of the anthracene moieties (Figure 5a).[8,10]

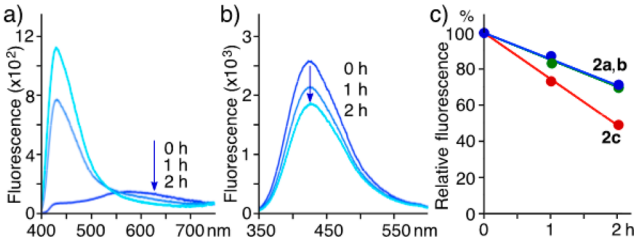

Figure 5. Fluorescence changes of (a) **2c** and (b) **2b**. (c) Time course of the emission intensities of **2a**–**c** in H_2O (1.0 mM based on the corresponding monomer) upon light irradiation (xenon lamp, 150 W m^{-2}, r.t., air).

However, the emission intensities of phenanthrene-embedded **2a** (at 400 nm) and naphthalene-embedded **2b** (at 424 nm) slightly decreased under similar conditions (Figures 5b and S54a). Kinetic analysis of the fluorescence changes revealed half-lives ($\tau_{1/2}$) of 3.4, 3.3, and 1.9 h for **2a**, **2b**, and **2c**, respectively (Figure 5c). Thus, capsules **2a**,**b** are stabilized toward UV light by ~2 times as compared with **2c**.

Finally, we revealed the host capability of **2a**–**c** and the fluorescent properties of the host–guest composites. A slight excess amount of coumarin-102 (**3**), a hydrophobic fluorescent dye, was added to H_2O solutions of **2a**–**c** (1.0 mM as based on **1a**–**c**). When the suspended solutions were stirred at room temperature for 1 h, clear pale-yellow solutions of **2a**–**c**⊃**3** were obtained after the removal of the suspended **3** by filtration. The UV–visible spectra exhibited new absorption bands at around 400 nm (Figure 6a), indicating that hydrophobic dye **3** is encapsulated in the inner hydrophobic space of hydrophilic hosts **2a**–**c**.[8,11] Upon irradiation of the host frameworks, host–guest composites **2a**,**b**⊃**3** showed blue emissions (λ_{max} = 480 nm) from bound **3** through efficient FRET from the host to the guest (Figure 6b). Interestingly, the emissive intensities of **2a**⊃**3** and **2b**⊃**3** further increased by 1.5 and 1.1 times, respectively, relative to those of the corresponding hosts without the guest (Figure 4e, green bars).[12]

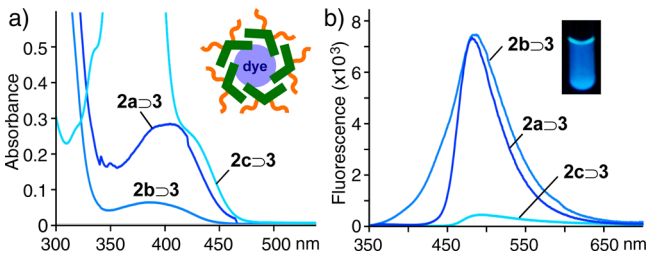

Figure 6. (a) UV–visible and (b) fluorescence spectra (r.t.) of **2a**–**c**⊃**3** in H_2O (1.0 mM based on **1a**–**c**). Excitation wavelengths: λ_{ex} = 297 nm for **2a**⊃**3**, λ_{ex} = 293 nm for **2b**⊃**3**, and λ_{ex} = 368 nm for **2c**⊃**3**.

In summary, we have shown for the first time fluorescent supramolecular capsules exhibiting an AIEE effect. The micelle-like nanocapsules were spontaneously and quantitatively formed in water at room temperature from V-shaped polyaromatic amphiphiles with phenanthrene or naphthalene rings. Notably, the emission intensities of the nanocapsules are higher than those of the monomeric amphiphiles (up to 2.5-fold) as well as that of the prototypical capsule with anthracene panels (up to 26-fold). Moreover, upon encapsulation of a fluorescent coumarin dye, the emission of the host–guest composites is enhanced as compared with that of the corresponding hosts. Further enhancement of the AIEE effect of the present photoactive nanocapsules and the investigation of unique host–guestf behavior in the polyaromatic cavities are now under study.

■ ASSOCIATED CONTENT

Supporting Information

Experimental procedures and physical properties. This material is available free of charge via the Internet at http://pubs.acs.org.

■ AUTHOR INFORMATION

Corresponding Author

*yoshizawa.m.ac@m.titech.ac.jp

Notes

The authors declare no competing financial interest.

■ ACKNOWLEDGMENTS

This work was supported by the Japan Society for the Promotion of Science (JSPS) through a "Funding Program for Next-Generation World-Leading Researchers (NEXT Program)" and by the Japanese Ministry of Education, Culture, Sports, Science and Technology (MEXT) through Grants-in-Aid for Scientific Research on Innovative Areas "Soft Molecular Systems". K.K. thanks JSPS for a Research Fellowship for Young Scientists.

■ REFERENCES

(1) Valeur, B.; Berberan-Santos, M. N. *Molecular Fluorescence: Principles and Applications*, 2nd ed.; Wiley-VCH Verlag & Co.: Weinheim, Germany, 2013.

(2) (a) Luo, J.; Xie, Z.; Lam, J. W. Y.; Cheng, L.; Chen, H.; Qiu, C.; Kwok, H. S.; Zhan, X.; Liu, Y.; Zhu, D.; Tang, B. Z. *Chem. Commun.* **2001**, 1740–1741. (b) Hong, Y.; Lam, J. W. Y.; Tang, B. Z. *Chem. Commun.* **2009**, 4332–4353. (c) Tang, B. Z.; Qin, A., Eds. *Aggregation-Induced Emission: Applications*; John Wiley & Sons: Chinchester, U.K., 2013.

(3) (a) Qin, A.; Lam, J. W. Y.; Jim, C. K. W.; Tang, B. Z. *Macromol. Symp.* **2009**, *279*, 7–13. (b) Qin, A.; Lam, J. W. Y.; Tang, L.; Jim, C. K. W.; Zhao, H.; Sun, J.; Tang, B. Z. *Macromolecules* **2009**, *42*, 1421–1424. (c) Tang, L.; Jin, J. K.; Qin, A.; Yuan, W. Z.; Mao, Y.; Mei, J.; Sun, J. Z.; Tang, B. Z. *Chem. Commun.* **2009**, 4974–4976. (d) Liu, J.; Zhong, Y.; Lam, J. W. Y.; Lu, P.; Hong, Y.; Yu, Y.; Yue, Y.; Faisal, M.; Sung, H. H. Y.; Williams, I. D.; Wong, K. S.; Tang, B. Z. *Macromolecules* **2010**, *43*, 4921–4936. (e) Wu, W.; Ye, S.; Yu, G.; Liu, Y.; Qin, J.; Li, Z. *Macromol. Rapid Commun.* **2012**, *33*, 164–171.

(4) (a) Hof, F.; Craig, S. L.; Nuckolls, C.; Rebek, J., Jr. *Angew. Chem., Int. Ed.* **2002**, *41*, 1488–1508. (b) Vriezema, D. M.; Aragonès, M. C.; Elemans, J. A. A. W.; Cornelissen, J. J. L. M.; Rowan, A. E.; Nolte, R. J. M. *Chem. Rev.* **2005**, *105*, 1445–1489. (c) Pluth, M. D.; Bergman, R. G.; Raymond, K. N. *Acc. Chem. Res.* **2009**, *42*, 1650–1659. (d) Yoshizawa, M.; Klosterman, J. K.; Fujita, M. *Angew. Chem., Int. Ed.* **2009**, *48*, 3418–3438. (e) Safont-Sempere, M. M.; Fernámdez, G.; Würthner, F. *Chem. Rev.* **2011**, *111*, 5784–5814. (f) Amouri, H.; Desmarets, C.; Moussa, J.

DOI: 10.1021/ja511463k
J. Am. Chem. Soc. 2015, 137, 98–101

Chem. Rev. **2012**, *112*, 2015−2041. (g) Cook, T. R.; Zheng, Y.-R.; Stang, P. J. *Chem. Rev.* **2013**, *113*, 734−777. (h) Smulders, M. M. J.; Riddell, I. A.; Browne, C.; Nitschke, J. R. *Chem. Soc. Rev.* **2013**, *42*, 1728−1754. (i) Yoshizawa, M.; Klosterman, J. K. *Chem. Soc. Rev.* **2014**, *43*, 1885−1898. (j) Zhang, G.; Mastalerz, M. *Chem. Soc. Rev.* **2014**, *43*, 1934−1947.

(5) Fluorescent coordination cages and capsules: (a) Al-Rasbi, N. K.; Sabatini, C.; Barigelletti, F.; Ward, M. D. *Dalton Trans.* **2006**, 4769−4772. (b) Harano, K.; Hiraoka, S.; Shionoya, M. *J. Am. Chem. Soc.* **2007**, *129*, 5300−5301. (c) Tidmarsh, I. S.; Faust, T. B.; Adams, H.; Harding, L. P.; Russo, L.; Clegg, W.; Ward, M. D. *J. Am. Chem. Soc.* **2008**, *130*, 15167−15175. (d) Li, Z.; Kishi, N.; Hasegawa, K.; Akita, M.; Yoshizawa, M. *Chem. Commun.* **2011**, *47*, 8605−8607. (e) Li, Z.; Kishi, N.; Yoza, K.; Akita, M.; Yoshizawa, M. *Chem.—Eur. J.* **2012**, *18*, 8358−8365. (f) Kishi, N.; Akita, M.; Yoshizawa, M. *Angew. Chem., Int. Ed.* **2014**, *53*, 3604−3607. (g) Neelakandan, P. P.; Jimenez, A.; Nitschke, J. R. *Chem. Sci.* **2014**, *5*, 908−915.

(6) Fluorescent micelle-like capsules with anthracene frameworks: (a) Kondo, K.; Suzuki, A.; Akita, M.; Yoshizawa, M. *Angew. Chem., Int. Ed.* **2013**, *52*, 2308−2312. (b) Suzuki, A.; Kondo, K.; Akita, M.; Yoshizawa, M. *Angew. Chem., Int. Ed.* **2013**, *52*, 8120−8123.

(7) Nonfluorescent micelle-like capsules: (a) Hiraoka, S.; Harano, K.; Shiro, M.; Shionoya, M. *J. Am. Chem. Soc.* **2008**, *130*, 14368−14369. (b) Hiraoka, S.; Harano, K.; Nakamura, T.; Shiro, M.; Shionoya, M. *Angew. Chem., Int. Ed.* **2009**, *48*, 7006−7009. (c) Hiraoka, S.; Nakamura, T.; Shiro, M.; Shionoya, M. *J. Am. Chem. Soc.* **2010**, *132*, 13223−13225.

(8) See the Supporting Information.

(9) DOSY NMR spectra of **2a**, **2b**, and **2c** in D_2O (2.0 mM) exhibited single bands at diffusion coefficients (D) of 2.6×10^{-10}, 4.3×10^{-10}, and 5.8×10^{-10} m^2 s^{-1}, respectively. The hydrodynamic diameters of the capsules were estimated to be 1.7 nm for **2a**, 1.1 nm for **2b**, and 0.8 nm for **2c** on the basis of the diffusion coefficient and the Stokes−Einstein equation.

(10) Becker, H.-D. *Chem. Rev.* **1993**, *93*, 145−172.

(11) The DLS analysis of host−guest composites **2a-c⊃3** in water (Figure S55) showed that the diameter of the composites are slightly larger (∼0.3 nm) than that of capsules **2a−c** (Figure S50a). ^{1}H NMR spectra of **2a,b⊃3** in D_2O revealed that the proton signals of the encapsulated dyes were significantly broadened owing to restriction of the molecular motion by the limited space of **2a,b** (Figure S58). The UV−visible analysis of **2a-c⊃3** revealed that each capsule contains one molecule of **3** within the polyaromatic shells in ∼80% yield for **2a,c** and ∼20% yield for **2b** based on $(\mathbf{1a-c})_5$.

(12) The quantum yields of **2a-c⊃3** include several factors such as FRET efficiency, AIEE/ACEQ effects, and host−guest ratio: Kondo, K.; Suzuki, A.; Akita, M.; Yoshizawa, M. *Eur. J. Org. Chem.* **2014**, 7389−7394.

DOI: 10.1021/ja511463k
J. Am. Chem. Soc. 2015, 137, 98−101